

Magneto spectroscopy of CdTe/Cd_{1-x}Mg_xTe modulation-doped quantum wells in THz and visible range

Jerzy Łusakowski^{1*}, Maciej Zaremba¹, Adam Siemaszko¹, Krzysztof Karpierz¹,
Zbigniew Adamus^{2,3}, Tomasz Wojtowicz³

¹ Faculty of Physics, University of Warsaw, Pasteura 5, 02-093 Warsaw, Poland

² Institute of Physics, Polish Academy of Sciences, Aleja Lotników 32/46, 02-668 Warsaw Poland

³ International Research Centre Mag Top, Institute of Physics, Polish Academy of Sciences, Aleja Lotników 32/46, 02-668 Warsaw, Poland

Article info

Article history:

Received 11 Oct. 2022

Received in revised form 03 Nov. 2022

Accepted 04 Nov. 2022

Available on-line 04 Apr. 2023

Keywords:

Terahertz spectroscopy; optically detected cyclotron resonance; modulation-doped CdTe quantum wells.

Abstract

Transport, photoluminescence, THz transmission, and optically detected cyclotron resonance studies were carried out on samples with a single modulation-doped CdTe/Cd_{1-x}Mg_xTe quantum well. THz experiments were performed at liquid helium temperatures for photon energies between about 0.5 meV and 3.5 meV. An effective mass of electron was determined to be $(0.1020 \pm 0.0003)m_0$. Observed photoluminescence and optically detected cyclotron resonance spectra cannot be explained within the simple model of Landau quantization of parabolic bands.

1. Introduction

Quantum wells (QWs) based on CdTe with Cd_{1-x}Mg_xTe barriers have been a subject of basic physics research for a few decades starting with the first report in 1993 [1]. Looking at the history of optical studies of this type of samples, two main paths of research can be noticed. The first one is related to the studies of trions, or charged excitons, mainly negatively charged. This research required a rather low concentration of free electrons in quantum wells, below about 10^{11} cm^{-2} , which allowed to clearly observe the spectrally narrow exciton and trion transitions [2]. The other path of research considered samples with a higher concentration of electrons, for which excitonic lines evolved into broad structures accompanied by the so-called Fermi edge singularity [3, 4]. Thus, for more heavily modulation-doped samples, interpretation of luminescence spectra is much more difficult because it requires consideration of many-body interactions. In fact, there are only a few research papers which go into details of the luminescence spectra of CdTe/Cd_{1-x}Mg_xTe with a high electron concentration [5].

Terahertz studies of CdTe/Cd_{1-x}Mg_xTe quantum structures have been focused so far on the cyclotron resonance and magnetoplasmonic resonances at frequencies of a few THz which required magnetic fields of about 10 T [6–8]. These studies allowed to determine in particular the dispersion of plasmons [6] and their polarization properties [7], or polaron-related nonlinearity of the cyclotron resonance at high magnetic fields [6, 8].

In the present paper, the authors focus on transmission experiments at low THz frequency of radiation (between 0.1 THz and 1 THz which corresponds roughly to the energy of photons from 0.4 meV to 4 meV) which allow to determine the effective mass of electron in the quantum wells studied. Next, photoluminescence measurements as a function of magnetic field allowed the authors to observe the Landau quantization with a clearly linear dependence of the position of luminescence peaks as a function of magnetic fields. However, it was shown that a description of these dependences cannot be made by a simple model assuming a constant effective mass of electrons and holes. Finally, the results of optically detected cyclotron resonance studies were presented, in which the cyclotron resonance was observed as a variation of luminescence intensity as a function of magnetic field.

*Corresponding author at: jerzy.lusakowski@fuw.edu.pl

2. Samples and experimental details

2.1. Samples and magnetotransport

The samples (named A, B, and C) used in the present experiment were grown with a molecular beam epitaxy. The magnesium content in barriers was equal to 0.2 which was determined from the photoluminescence (PL) spectra [9]. Sample A contained a 15 nm wide single QW, while the width of a QW in samples B and C was equal to 20 nm. Results of the magnetotransport measurements for sample B and C are shown in Fig. 1 and Fig. 2, respectively. Data for sample A are similar once a background related to a parallel conductance is subtracted. Resulting concentration (n_s) and mobility of a two-dimensional electron gas (2DEG) in these samples are shown in Table 1. These data are given for samples cooled in the dark and after subsequent illumination, which leads to an increase in 2DEG concentration and mobility.

Table 1.
2DEG concentration and mobility at 1.4 K before and after illumination with 514 nm light.

Sample	Mobility ($10^5 \text{ cm}^2/\text{Vs}$)		Concentration (10^{11} cm^{-2})	
	Dark	After illumination	Dark	After illumination
A	1.4	2.6	4.6	5.4
B	0.9	2.5	2.6	3.5
C	1.3	2.6	4.5	5.6

The high quality of the samples allows to observe the quantum Hall effect in all of them.

2.2. Experimental systems

THz radiation transmission was studied with samples placed in a variable temperature insert in pumped liquid helium cooled to about 1.8 K. The source of radiation was a backward wave oscillator working in its basic frequency range between about 0.1 THz and 0.17 THz and supplied with frequency multipliers ($\times 2$, $\times 3$, and $\times 6$). This set-up allowed to cover the range of frequency from about 0.1 THz up to 1 THz. The radiation was delivered to the sample with a stainless steel tube (inner diameter equal to 17 mm) which ended with a crystalline quartz lens and a brass cone reducing the tube diameter to 4 mm. The sample studied was adjacent to the exit port of the cone. Transmitted signal was detected with a thinned Allan-Bradley resistor placed just below the sample. The detector electrical circuit consisted of a sensor, a load resistor, and a voltage source working at 10 V. Under experimental conditions, the resistance of the sensor was equal to about 100 k Ω and the resistance of the load was 130 k Ω . The radiation was chopped with a mechanical beam modulator at 4 Hz and the AC signal appearing on the load resistor was registered with a lock-in amplifier. The sample was placed in the centre of a superconducting coil generating magnetic fields up to 10 T. Measurements were carried out as a function of magnetic field by sweeping the coil current typically with a speed of 0.05 A/s or 0.1 A/s. Generally, spectra were measured sweeping the magnetic field up and

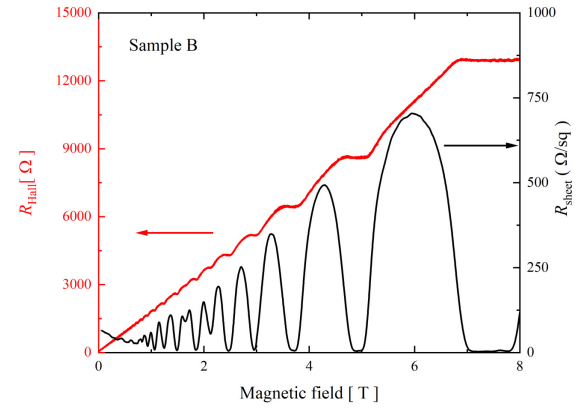


Fig. 1. Hall resistance (red curve, left scale) and Shubnikov-de Haas resistance (black curve, right scale) for sample B at 1.7 K.

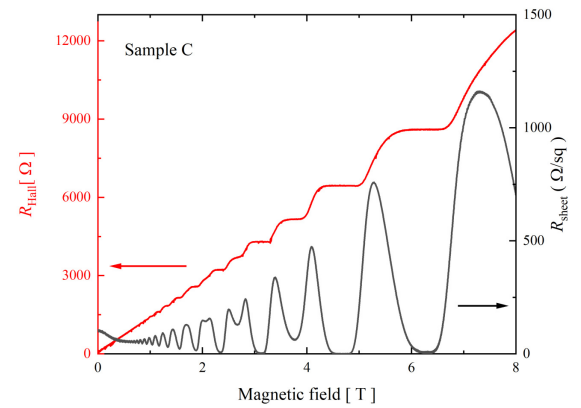


Fig. 2. Hall resistance (red curve, left scale) and Shubnikov-de Haas resistance (black curve, right scale) for sample C at 1.7 K.

down to account for possible shifts resulting from the coil inductance and resistance of a protection circuit.

The same insert could be simultaneously used to carry out measurements in the range of visible light to study PL. In this case, the authors used an Ar⁺ laser (the wavelength equal to 514 nm) and PL was measured with an Acton spectrometer supplied with a CCD camera. The laser light was passing through the tube as a free beam and was focused on a sample with the lens which was placed at about 3 cm from the sample. The lens also served as a cold filter which cut THz radiation emitted by parts of the system which were at room temperature.

Most of spectroscopic measurements presented in this work were carried out on sample A. Samples B and C were tested in transport and THz transmission to verify whether the parallel conductance changes the position of the cyclotron resonance. In the case of samples A and C, position (i.e., the resonant magnetic field, B_{CR}) of the cyclotron resonance was measured both before and after illumination.

3. Results and discussion

3.1. The cyclotron resonance

The transmission of THz radiation was registered as a function of magnetic field. An example set of transmission curves is shown in Fig. 3. The magnetic field corresponding

to the minimum of the transmission curve was interpreted as the cyclotron resonance field. Repeating such measurements for all samples before and after illumination allowed to obtain a set of data which is presented in Fig. 4.

Figure 4 shows that there is no measurable difference in position of the cyclotron resonance for samples before and after illumination and all data points follow the same linear dependence on the magnetic field. The slope of the thin red line is given by $2\pi m_e/h_e$, where e and m_e are the charge and the effective mass of electron, respectively, and h is the Planck constant. Basing on the data presented in Fig. 4, the authors determined $m_e/m_0 = 0.1020 \pm 0.0003$, where m_0 is the free electron mass. This result is in full agreement with earlier studies of the cyclotron mass in CdTe-based quantum wells of the width equal to 15 nm and 20 nm (see Fig. 3 in Ref. 8). It should be indicated that the value of the effective mass here determined is higher than that found in bulk n-CdTe crystals in Ref. 10. It should be noted that spatial confinement shifts the energy electron levels up in the quantum wells, which increases their mass due to non-parabolicity. On the other hand, this increase (in comparison with the bulk material) should not be related to the presence of non-equilibrium electrons because their concentration is orders of magnitude lower than that resulting from modulation doping.

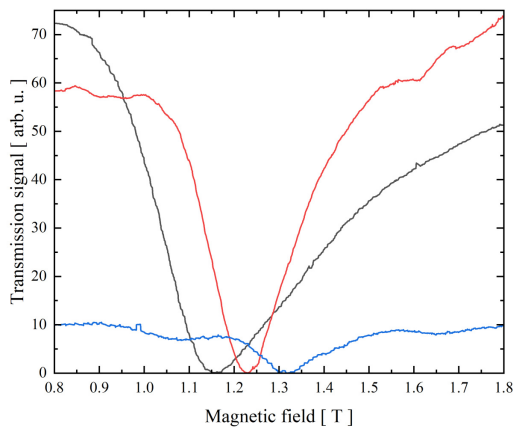


Fig. 3. Intensity of radiation transmitted through sample A. The energy of THz photons is 1.32, 1.39, and 1.49 meV for black, red, and blue curves, respectively. The data are not normalized to the power of the THz source.

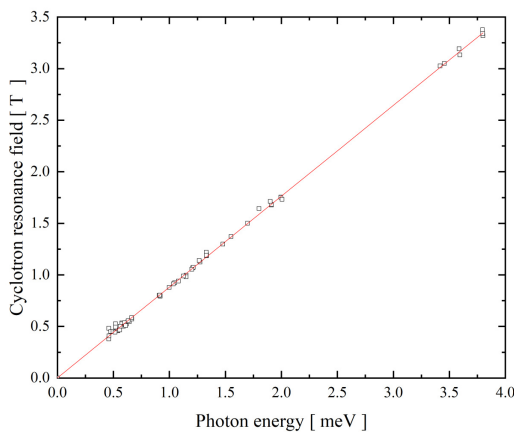


Fig. 4. Dependence of the cyclotron resonance field on energy of photons. The figure collects the data obtained on samples A, B, and C before and after illumination. The thin red line is a linear fit to data points.

As can be seen from Table 1, illumination of samples leads to an increase of the 2DEG concentration below about $6 \times 10^{11} \text{ cm}^{-2}$, a concentration for which non-parabolicity effects are not important. Also, the energy of photons used in the experiment is too low to shift the resonance magnetic field towards the region of about 10 T where the non-linearity of the cyclotron resonance appears due to the interaction of electrons with optical phonons [6, 10].

3.2. Magnetophotoluminescence

Figure 5 presents the results of a photoluminescence study of sample A in a narrow range of magnetic field where a wavy nature of the shape of the spectra can be observed. Deconvolution into Lorentzian peaks (an example is shown in Fig. 6) reveals luminescence originating from transition between Landau levels in the conduction and valence bands.

The linear dependence of the position of luminescence peaks visible in the spectra presented in Fig. 5 on magnetic field suggests that they result from optical transitions between Landau levels in the conduction and valence bands. In a simple model, the magnetic field dependence on transition between these levels can be expressed as

$$E = E_0 + \left(n + \frac{1}{2}\right) \hbar eB \left(\frac{1}{m_e} + \frac{1}{m_h}\right), \quad (1)$$

where E_0 is the energy separating the electron and hole ground states in the quantum well, n is the number of Landau levels involved in the transition, and m_h is the hole effective mass. The selection rule of $\Delta n = 0$ is applied in

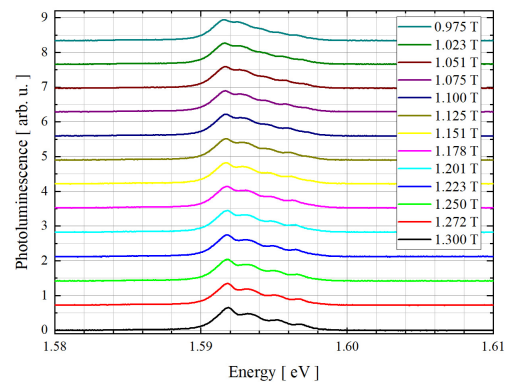


Fig. 5. Photoluminescence spectra of sample A at indicated magnetic fields. The spectra are vertically shifted for clarity.

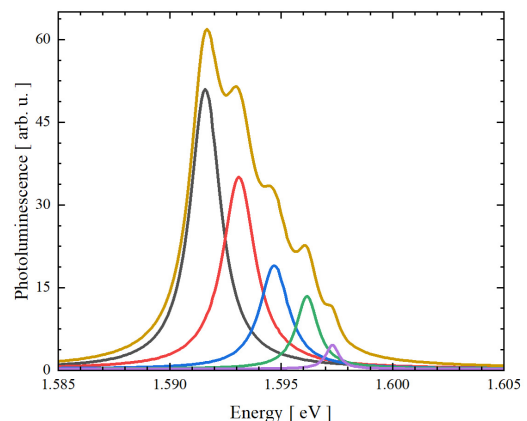


Fig. 6. Example of the deconvolution of a spectrum measured at $B = 1.223 \text{ T}$ for sample A into Lorentzian peaks.

the above formula, i.e., the luminescence transition occurs between the electron and hole Landau levels of the same number n .

Data presented in Fig. 4 give a precise value of the effective mass of electron which can be used in (1) to determine the effective mass of the hole when the equation is applied to the data presented in Fig. 7. However, one is then confronted with the values of m_h varying between $0.13 m_0$ and $0.61 m_0$, which shows that the model leading to (1) cannot be applied in this case.

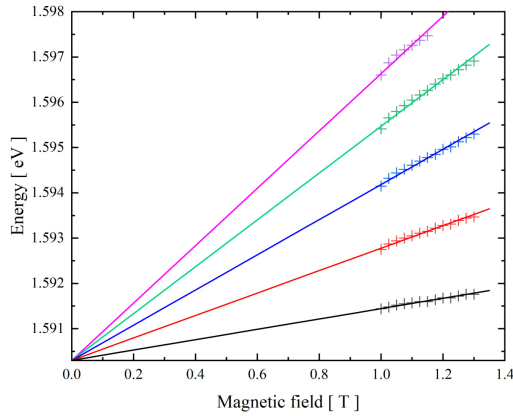


Fig. 7. Dependence of the position of Lorentzian peaks as a function of magnetic field. The points presented in the figure result from the deconvolution of the spectra presented in Fig. 6

Seeking an explanation for this result, reference was made to calculations of the energy of optical transitions in a GaAs-based QW [11]. Similar calculations should be carried out in the case of the present paper, however, this is beyond its scope (see the next paragraph for a more detailed discussion of this point).

It should be noted that the Landau-level-related maxima in the PL spectra presented in Fig. 5 come from the quantization of the equilibrium density of populated states and not from the population of higher levels by illumination of the sample with laser light. The argument supporting this statement stems from the width of PL spectra which is equal to about 10 meV (see Fig. 5). Position of the Fermi level with respect to the ground state in the conduction band of the QW, given by $\hbar^2 n_s / 4\pi m_e$ for the parabolic and spherical bands, gives a value of 12.5 meV for a concentration of $5.4 \times 10^{11} \text{ cm}^{-2}$, which is close to the width of the observed spectra. Also, the observation of luminescence from Landau levels occupied only with non-equilibrium electrons would require time-resolved measurements with a picosecond resolution due to a fast relaxation of electrons to the ground state in the conduction band.

3.3. Optically detected cyclotron resonance

The authors used the capabilities of the experimental system to detect the cyclotron resonance by monitoring luminescence. At several values of magnetic field, PL spectra were measured with and without THz radiation with a photon energy equal to 1.39 meV. One set of these curves (with THz radiation off) is presented in Fig. 5. Having another set of curves for THz radiation on, the difference of the corresponding curves which led to the

optically detected cyclotron resonance (ODCR) was calculated and the data are presented in Fig. 8.

The procedure to obtain the ODCR spectra (“THz off” spectra subtracted from “THz on” spectra) means that a decrease/increase of the intensity in ODCR spectrum indicates a decrease/increase in the intensity of the PL itself under the influence of THz radiation. Generally, the ODCR spectra show a minimum at about 1.592 eV which is close to the PL peak of the lowest energy in Fig. 5 and corresponds to transitions between electrons and holes in the lowest Landau levels in the conduction and valence bands. A shallow minimum is also observed at about 1.593 eV, which evolves into a broad maximum extending between about 1.593 eV and 1.598 eV, in the region of transitions between the Landau levels with higher indexes. This maximum does not show an internal structure except in a resonant magnetic field of 1.223 T (blue curve in Fig. 8 marked CR) for which clearly visible maxima are present. The crosses in Fig. 8 show the positions of luminescence maxima visible in Fig. 5. It can be noticed that the crosses do not coincide with the extrema of the luminescence although they are close to them.

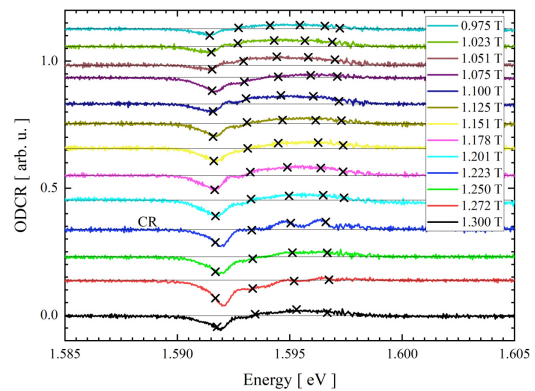


Fig. 8. ODCR data obtained at a photon energy equal to 1.39 meV at several values of magnetic field (indicated). The curve which is marked CR corresponds to a resonant magnetic field of 1.223 T. Crosses mark the positions of PL peaks visible in the spectra in Fig. 5. The spectra are vertically shifted. Thin horizontal lines show the zero value of the signal.

It should be noted that the cyclotron resonance in the investigated samples leads to a rather broad line as a function of magnetic field (see Fig. 3), which allows to understand why the ODCR signal is observed in a rather broad range of magnetic field. The ODCR signal, as the luminescence itself, comes from transitions which involve Landau levels both in the conduction and valence bands and – as it was mentioned above – a detailed analysis of the energy of these transitions requires an advanced modelling.

To be more specific, the authors briefly describe the solution of a similar problem which considered two-dimensional hole Landau levels in a p-typed modulation-doped $\text{Al}_x\text{Ga}_{1-x}\text{As}/\text{GaAs}$ heterostructures [11]. The similarities of that case to our problem are the following: a) in both cases, modulation-doped systems with a built-in electric field coming from ionized impurities are considered; b) only direct band materials of the zinc-blende structure are considered and the analysis is restricted to the vicinity of the Γ point in the Brillouin zone; c) quantization

of the Γ_8 valence band in the magnetic field is one of the main subjects of interest.

The model presented in Ref. 11 is based on the Luttinger Hamiltonian (4×4 matrix) [12], the elements of which change when passing from one layer to another. Also, the electrostatic potential of the heterostructure, resulting from the self-consistent Schrodinger-Poisson calculations, is taken into account. Appropriate boundary conditions on the heterointerfaces allow to numerically calculate holes wave functions as a function of their k -vector and magnetic field. Although the method of calculations is clearly presented in Ref. 11, passing through this numerical recipe is a project in itself, which is left for further study.

4. Conclusions

In conclusion, the authors carried out transport, luminescence, THz transmission, and optically detected cyclotron resonance studies of single CdTe/Cd_{1-x}Mg_xTe quantum wells. The experiments were carried out at liquid helium temperatures for a THz photon energy between about 0.4 meV and 4 meV. In THz transmission measurements, samples with and without parallel conductance and before and after illumination with a laser green light were studied. It was shown that neither the parallel conductance nor illumination-induced changes in 2DEG concentration and mobility influence the position of the cyclotron resonance. Fitting to the data allowed to determine the effective mass of electron to be $(0.1020 \pm 0.0003)m_0$. Luminescence spectra showed the Landau quantization of the electron and hole levels, however, interpretation of the energy dependence on the transitions as a function of magnetic field requires prior modelling. Also, the shape of the observed ODCR signal cannot be explained without a deeper connection to the numerical model.

Authors' statement

Research concept, data collection and treatment, writing the article: J.Ł., data collection and treatment: M.Z., A.S., K.K., and Z.A.; growth of samples: Z.A and T.W.

Acknowledgements

This research was partially supported by the Polish National Science Centre grant UMO-2019/33/B/ST7/02858 and by the Foundation for Polish Science through the IRA Programme co-financed by EU within SG OP (Grant No. MAB/2017/1).

References

- [1] Kuhn-Heinrich, B. *et al.* Optical investigation of confinement and strain effects in CdTe/(CdMg)Te quantum wells. *Appl. Phys. Lett.* **63**, 2932–2934 (1993). <https://doi.org/10.1063/1.110277>
- [2] Kheng, K. *et al.* Observation of negatively charged excitons X in semiconductor quantum wells. *Phys. Rev. Lett.* **71**, 1752–1755 (1993). <https://doi.org/10.1103/PhysRevLett.71.1752>
- [3] Wojtowicz, T. *et al.* Novel CdTe/CdMgTe graded quantum well structures. *Acta Phys. Pol.* **92**, 1063–1066 (1997). <http://przyrbwn.icm.edu.pl/APP/PDF/92/a092z5p48.pdf>
- [4] Huard, V. *et al.* Magneto-optical absorption studies of modulation-doped CdTe and CdMnTe quantum wells. *Phys. Status Solidi A* **178**, 95–99 (2000). [https://doi.org/10.1002/1521-396X\(200003\)178:1<95::AID-PSSA95>3.0.CO;2-V](https://doi.org/10.1002/1521-396X(200003)178:1<95::AID-PSSA95>3.0.CO;2-V)
- [5] Kunc, J. *et al.* Enhancement of the spin gap in fully occupied two-dimensional Landau levels. *Phys. Rev. B* **82**, 115438 (2010). <https://doi.org/10.1103/PhysRevB.82.115438>
- [6] Grigelionis, I. *et al.* Magnetoplasmons in high electron mobility CdTe/CdMgTe quantum wells. *Phys. Rev. B* **91**, 075424 (2015). <https://doi.org/10.1103/PhysRevB.91.075424>
- [7] Yavorskiy, D. *et al.* Polarization of magneto plasmons in grating metamaterial based on CdTe/CdMgTe quantum wells. *Materials* **13**, 1811 (2020). <https://doi.org/10.3390/ma13081811>
- [8] Karczewski, G., Wojtowicz, T., Wang, Y.-J., Wu, X. & Peeters, F. M. Electron effective mass and resonant polaron effect in CdTe/CdMgTe quantum wells. *Phys. Status Solidi B* **229**, 597–600 (2002). [https://doi.org/10.1002/1521-3951\(200201\)229:1<597::AID-PSSB597>3.0.CO;2-P](https://doi.org/10.1002/1521-3951(200201)229:1<597::AID-PSSB597>3.0.CO;2-P)
- [9] Ossau, W. *et al.* Cd_{1-x}Mg_xTe: a new promising barrier material to CdTe based heterostructures. *Superlattices Microstruct.* **16**, 5–10 (1994). <https://doi.org/10.1006/spmi.1994.1099>
- [10] Helm, M. *et al.* Polaron cyclotron resonance in n-CdTe and n-InP. *Solid State Comm.* **53**, 547–550 (1985). [https://doi.org/10.1016/0038-1098\(85\)90189-9](https://doi.org/10.1016/0038-1098(85)90189-9)
- [11] Kubisa, M. *et al.* Photoluminescence investigations of two-dimensional hole Landau levels in p-type single Al_xGa_{1-x}As/GaAs heterostructures. *Phys. Rev. B* **67**, 035305 (2003). <https://doi.org/10.1103/PhysRevB.67.035305>
- [12] Luttinger, J. M. & Kohn, W. Motion of electrons and holes in perturbed periodic fields. *Phys. Rev.* **97**, 869–883 (1955). <https://doi.org/10.1103/PhysRev.97.869>